

## Design and evaluation of a distributed TDR moisture sensor

Bin Zhang<sup>a</sup>, Xinbao Yu<sup>a</sup> and Xiong Yu<sup>\*b</sup>

*Department of Civil Engineering, Case Western Reserve University, 10900 Euclid Avenue,  
Bingham 203B, Cleveland, OH 44106-7201, USA*

(Received June 11, 2009, Accepted April 29, 2010)

**Abstract.** This paper describes the development and evaluation of an innovative TDR distributed moisture sensor. This sensor features advantages of being responsive to the spatial variations of the soil moisture content. The geometry design of the sensor makes it rugged for field installation. Good linear calibration is obtained between the sensor measured dielectric constant and soil physical properties. Simulations by the finite element method (FEM) are conducted to assist the design of this sensor and to determine the effective sampling range. Compared with conventional types of moisture sensor, which only makes point measurement, this sensor possesses distributed moisture sensing capability. This new sensor is not only easy to install, but also measures moisture distribution with much lower cost. This new sensor holds promise to significantly improve the current field instruments. It will be a useful tool to help study the influence of a variety of moisture-related phenomena on infrastructure performance.

**Keywords:** TDR; strip sensor; moisture distribution; distributed; FEM; field instrument; sensor; infrastructure.

---

### 1. Introduction

Water is one of the most important factors causing the deterioration of infrastructures. Water accumulated behind retaining walls compromises their structural stabilities. Seepage through levees and earth dams can lead to piping. Moisture migration under pavements needs to be controlled through proper drainage design. The accumulation of moisture in pavement structures has been identified to be a major cause of pavement distress despite of improvement in mix design (Huang 2003, Graf and Zink 2005). According to the Asphalt Institute, moisture-related damage accounts for 60% of pavements distress. Moisture related problems prevail among the more than 2.5 million miles of paved roads in the United States (Liang *et al.* 2006, example shown in Fig. 1(a)). It also combines with local geological conditions such as expansive soils and freeze/thaw susceptible subgrade to cause distress in special geographic regions (Hong *et al.* 2006, Salem *et al.* 2003). The annual cost for mitigating moisture related damage is estimated in billions of dollars (Abo-Hashema *et al.* 2002). Moisture migration can also cause transport of contaminants under the ground. Besides, high moisture is generally associated with severe corrosive environment; this causes higher rate of corrosion for the underground pipelines, storage tanks and metal anchors (i.e., Fig. 1(b)). Moisture is

---

<sup>\*</sup>Corresponding Author, Assistant Professor, E-mail: xiong.yu@case.edu

<sup>a</sup>Graduate Assistant

<sup>b</sup>Assistant Professor



Fig. 1 Examples of moisture-caused infrastructure deterioration: (a) pavement, (b) underground pipe and (c) bridge (stray cable)

also the dominating factor for the corrosion of bridges; for example, prevention of moisture infiltration in the cables is an important task for cable-stay bridges and suspension bridges (i.e., Fig. 1(c)). Infiltration of moisture and chloride salt is the major source causing the corrosion of steel rebars in bridge deck. Sensors to real time monitoring the spatial and temporal distribution of moisture along these critical infrastructures would provide important warning signals where proper corrective actions can be taken. In summary, monitoring the distribution of moisture has wide engineering implications.

Sensors based on Time Domain Reflectometry (TDR) are currently the most commonly used for monitoring soil water content in the field. TDR sensors feature advantages such as being rugged, accurate and inexpensive. Most of current TDR sensors, however, only measure the moisture content at a single location. It requires multiplexing of multiple sensors to measure its spatial distribution. Besides, the installation procedures are cumbersome, for example, when installing under existing pavements. Their reliability can also be compromised due to soil disturbance over a large area. This paper describes the development and evaluation of an innovative distributed TDR moisture sensor, which aims to overcome the shortcomings of the existing TDR sensors. This strip sensor utilizes inexpensive metal strips of selected length (depending on application requirements) aligned with controlled geometry. Experimental data indicates it has high sensitivity to the spatial moisture distribution along the sensor. The performance of this strip sensor is also evaluated under simulated laboratory tests. Experience of field installation indicates the new strip sensor is much easier to install than conventional types of TDR sensor.

## 2. Background

### 2.1 Time Domain Reflectometry

Time Domain Reflectometry (TDR) is an established technology for measuring the soil water content. It is widely used for geotechnical applications. Fig. 2 shows a typical TDR system, which typically includes a TDR apparatus, a coaxial cable and a sensing probe. To make measurement, TDR device generates a fast-rising electrical pulse, which travels along the measurement system. Reflections occur at interfaces where material properties change. These are recorded by TDR sampling unit. From the TDR signal, the travel speed of electromagnetic wave,  $v$ , in a material can be determined. This is used to calculate an electromagnetic property called apparent dielectric

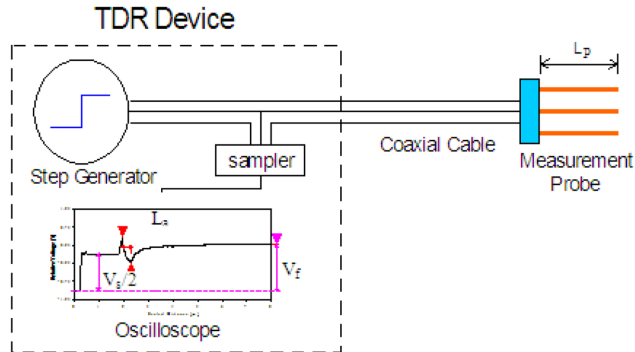


Fig. 2 Schematic of a TDR system and output signal (Yu and Drnevich 2004)

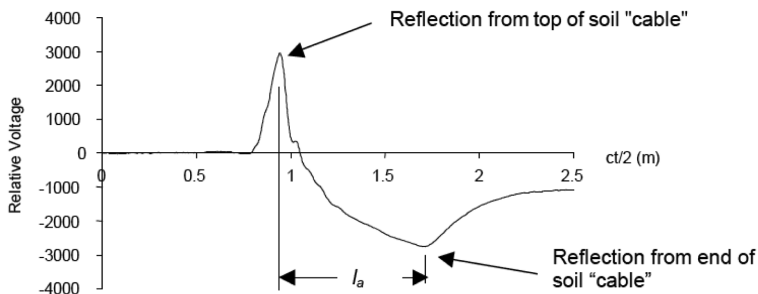


Fig. 3 A typical TDR curve for soil and the measurement of apparent length  $l_a$  (Drnevich *et al.* 2001a)

constant,  $K_a$ , by Eq. (1) (Drnevich *et al.* 2001b, O'Connor and Dowding 1999, Yu and Drnevich 2004)

$$v = \frac{c}{\sqrt{K_a}} \quad (1)$$

where  $c$  is the velocity of an electromagnetic wave in free space ( $2.988 \times 10^8$  m/s).

Schematic of calculating the dielectric constant  $K_a$  is given in Fig. 3. It is from the round trip time of electromagnetic wave travelling along the embedded TDR probe via Eq. (2)

$$K_a = \left( \frac{l_a}{L} \right)^2 \quad (2)$$

where  $l_a$  is the apparent length, which is determined from the time elapse between reflections as illustrated in Fig. 3.  $L$  stands for the length of the TDR probe (Yu and Yu 2006, Liang *et al.* 2006, Wörsching *et al.* 2006, Schlaeger *et al.* 2001).

The dielectric constants of soils are strongly related to their water contents, since water has a much larger dielectric constant (around 81 at 20 °C) than that of soil solid (around 3 to 5) or air (1). A variety of formulas have been developed to establish quantitative relationships (Topp *et al.* 1980, Siddiqui and Drnevich 1995). Eq. (3) is unique in that it uses the concept of gravimetric water content and explicitly accounts for the effects of soil dry density.

$$\sqrt{K_a} \frac{\rho_w}{\rho_d} = a + bw \quad (3)$$

where  $K_a$  is the TDR measured dielectric constant,  $\rho_w$  is the density of water,  $\rho_d$  is the dry density of soil, a and b are constants dependent upon a specific soil type,  $w$  is the gravimetric water content.

TDR possess the capability of distributed measurements since the signal accumulates information as electromagnetic waves travel along the metallic waveguide. Such distributive sensing capability has been explored both conceptually and experimentally for strain measurement (Stastny *et al.* 1993, Lin *et al.* 1997, Tang *et al.* 2001). Chen *et al.* (2004) demonstrated an electrical TDR coaxial cable sensor for detection of structural damage and crack/strain recording. The innovatively designed sensor showed very high sensitivities and resolution for detecting cracks in concrete. Lin *et al.* (2005) also introduced a prototype coaxial ETDR cable sensor for distributive strain measurements. Schlaeger *et al.* (2001), and more recently, Wörsching *et al.* (2006) described a flat strip moisture sensor developed in Europe. Promising results were obtained with the sensor prototypes, although the sensitivity in the sensor remains to be improved.

Innovative design of TDR sensor is required to utilize the advantages of TDR for distributive measurement. Traditional TDR sensors only measure the bulk material behaviors. In the case of soils, materials are assumed to be uniform over the TDR probe length. Variations of soil properties along the probe cause additional reflections and are treated as nuisance signals. By improving the sensor design and methods for signal analyses, these fine details can be utilized to support engineering decisions.

## 2.2 Sensor design and evaluation

### 2.2.1 Design of a strip TDR sensor

A new coplanar strip TDR sensor is designed to be suitable for installation under pavement subgrade for long term monitoring the moisture distribution in any specified direction. The sensing cable is made of steel strips to provide waveguide for electromagnetic waves (Fig. 4). The electrical

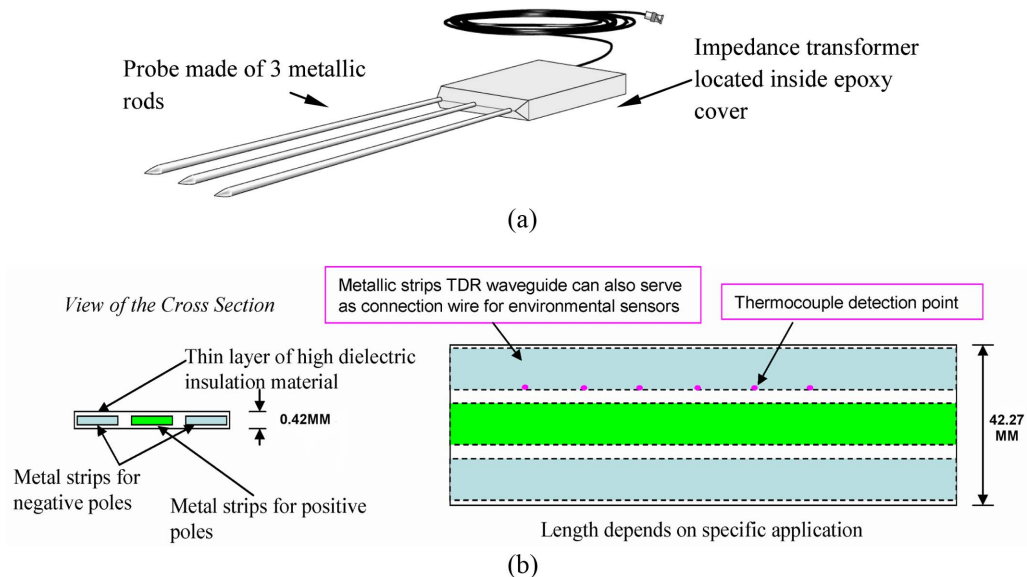


Fig. 4 (a) Schematic of 3-rod TDR probe by Campbell Scientific Inc. and (b) schematic TDR flat cable sensor design: left) cross section; right) view of the cable

criteria ensures that the sensor is sensitive and accurate for large globalized measurement. These have to be achieved by satisfying two important requirements in sensor design.

### 2.2.1.1 Providing sufficient sampling volume while maintaining desired frequency mode

For soils with maximum particle size around 9.5 mm, standard (ASTM D2216) recommends a minimum sample of 500 g to achieve a water content measurement accuracy of  $\pm 0.1\%$ . Larger amounts of sample is needed for soils with larger particles. Referring to the experience with parallel rod transmission line (Topp and Davis 1985, Baker and Allmaras 1990, Zegelin *et al.* 1989), the sampling range normal to the sensor probe is approximately 1.4 to 1.7 times the probe spacing. A larger sampling zone can be achieved by increasing the spacing between the strips.

On the other hand, increasing the distance between sensor strips reduces the cut-off frequency above which electromagnetic wave in non-TEM (Transverse ElectroMagnetic) modes start to propagate (Ramo *et al.* 1994). Besides, it is necessary to restrain the geometry of the coplanar strip sensor to maintain high effective measurement frequency (for example, in low GHz range). Since soils are generally highly dispersive, maintaining high effective measurement frequency will make the measurement results to be less influenced by factors such as soil type or pore fluid characteristics (Yu and Drnevich 2004). The geometry of the sensor has to be optimized by considering both factors.

### 2.2.1.2 Preventing signal attenuation while maintaining sensitivity

Electromagnetic wave is attenuated when propagating in conductive materials like soils. This limits the length of the TDR sensor that can be installed for monitoring purpose. Coating TDR probe with an insulating material has been proven to be effective in preventing energy loss (Mojid *et al.* 1998, Nichol *et al.* 2002, Persson *et al.* 2004). The use of insulations such as by epoxy, plastic wrap or adhesive tapes have low dielectric constants. This results in the reduction in the sensitivity for a coated TDR sensor probe. This can be observed in Fig. 5. The x-axis of this figure is the dielectric constant measured by a plain TDR probe. The y-axis is the dielectric constant measured by a coated TDR probe. The group of curves show the effects of the dielectric constant of the

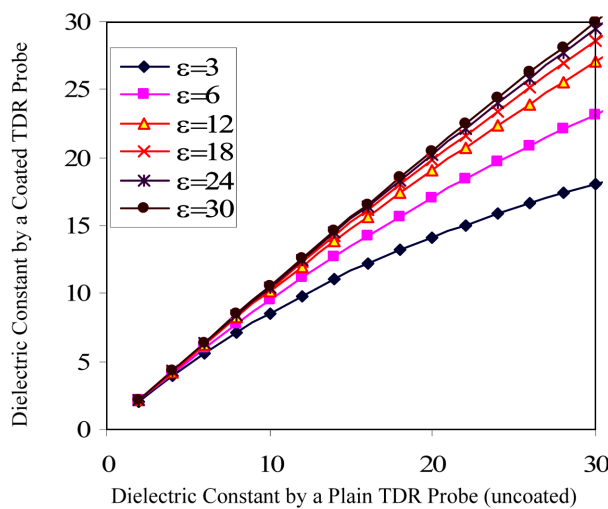


Fig. 5 The effects of coating on the dielectric constants by coated probe ( $\epsilon$  is the dielectric constant of coating, after Yu 2003)

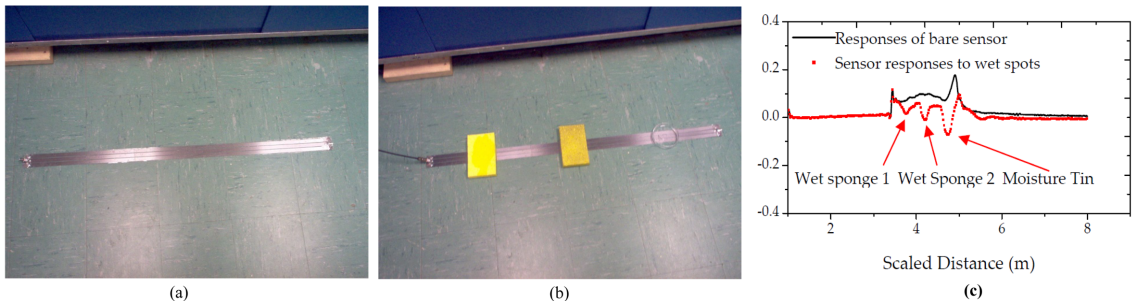


Fig. 6 (a) Photo of TDR strip distributive moisture sensor, (b) TDR distributive moisture sensor with artificial wet spots and (c) TDR signals for strip sensor and for strip sensor with artificial wet spots

coating material (Fig. 4(b)). The curves are generated using a dielectric model for composite material by Yu (2003). Fig. 5 showed that the measured dielectric constants by a coated probe were generally smaller than the dielectric constant measured by a plain uncoated TDR probe. Therefore, the sensitivity of an insulated TDR probe is reduced compared with a plain TDR probe. Proper calibration would be necessary to obtain the actual dielectric constant for a given material.

### 2.2.2 Sensor fabrication and evaluation

The strip TDR sensor developed in this study is made of three inexpensive stainless steel strips accurately aligned to be parallel. The metal strip is made of high-carbon steel with 12.5 mm wide and 0.254 mm thick. The metal strips are separated by a 2 mm gap. This gap is filled with Polytetrafluoroethylene (PTFE) Teflon. The top and bottom surface are covered with tape. With the assigned width and spacing of the steel strips, the TDR strip sensor has an electric impedance of 50 ohm when it is exposed in air. The total material cost is less than \$100 for a 5 ft strip TDR sensor. Fig. 6(a) shows the photos of fabricated strip sensor. The flat geometry of the strip sensor makes it easily placed horizontally compared with conventional TDR rod (Fig. 4(a) versus Fig. 6(a)). The length of the TDR strip sensor can be fabricated according to application requirements. The longest one we have fabricated so far is 45 ft in length.

Fig. 6(c) shows the recorded TDR signals for bare strip and for strip with artificial wet spots placed along the strip. Comparison of both signals indicates that the wet spots cause distinctive reflections in the recorded TDR signal. This is an indication that the TDR strip has good sensitivity.

### 2.2.3 The effective sensor sampling area

#### 2.2.3.1 Theoretical basis

The effective sampling area by the sensor is studied by use of Finite Element Simulations by use of the concept of the effective dielectric constant. For Transverse Electromagnetic (TEM) Wave, the electrical field in the plane perpendicular to the direction of wave propagation can be treated as electrostatic field. The electrical potential is described by the Poisson's equation (Eq. (4)).

$$\nabla \cdot (\epsilon \nabla V) = -\rho \quad (4)$$

where  $\epsilon$  is the dielectric permittivity, which is a function of space coordinates;  $V$  is the electrical potential;  $\rho$  is the space charge density in medium surrounding waveguide and is assumed to be 0 for metallic waveguide.

The electrical potential is related to the strength of electrical field  $\vec{E}$

$$\vec{E} = \nabla V \quad (5)$$

The TDR sensor measures the effective dielectric constant of heterogeneous materials around the sensor in the plane perpendicular to the direction of EM wave propagation. The effective dielectric constant is the spatial weighted average of the dielectric constant (Knight 1992).

$$K_{a,e} = \iint_{\Omega} K_a(x,y) s(x,y) dA \quad (6)$$

where  $K_a(x,y)$  is a function of the distribution of the dielectric constant around TDR waveguide;  $s(x,y)$  is the spatial weighting function.  $\Omega$  is the total area contributing to the electrical energy field.

The weighing function is determined based on the concept of equivalence in the electric field energy. Eq. (7) gives the stored energy per unit length,  $W$ , of a TDR waveguide installed in heterogeneous materials (Knight 1992).

$$W = \frac{1}{2} \varepsilon_0 \iint_{\Omega} K_a(x,y) |\vec{E}(x,y)|^2 dA \quad (7)$$

where  $\varepsilon_0$  is the dielectric permittivity of free space;  $E$  is the electric field intensity, which can be determined by solving the Poisson's equation with FEM.

Eq. (8) gives the stored energy per unit length,  $W$ , of a TDR waveguide installed in homogeneous material of dielectric constant  $K_{a,e}$  (Knight 1992).

$$W = \frac{1}{2} \varepsilon_0 \iint_{\Omega} K_{a,e} |\vec{E}_0(x,y)|^2 dA \quad (8)$$

$\varepsilon_0$  is the electric field intensity for strip in vacuum (dielectric constant of 1).

Combining Eqs. (7) and (8), the effective dielectric constant  $K_{a,e}$  is

$$K_{a,e} = \frac{\iint_{\Omega} K_a(x,y) |\vec{E}(x,y)|^2 dA}{\iint_{\Omega} |\vec{E}_0(x,y)|^2 dA} \quad (9)$$

Comparing Eqs. (9) and (6), the spatial weighting function is given by

$$s(x,y) = \frac{|\vec{E}(x,y)|^2}{\iint_{\Omega} |\vec{E}_0(x,y)|^2 dA} \quad (10)$$

The effective sampling area of TDR probe is determined from the spatial weighing function and its relative contribution to the total values. Ferré *et al.* (1998) presented a method based on the spatial weighting function, i.e., Eq. (11), to calculate the effective sampling area of a TDR probe.

$$f = \frac{100 \times \sum_{i=1}^n s_i(x,y) A_i}{\sum_{i=1}^N s_i(x,y) A_i} \quad (11)$$

where  $A_i$  is the area of an element,  $s_i$  is its corresponding weighting function,  $n$  is the number of element used for summation,  $N$  is the total elements in the computational domain.  $f$  is the percent contribution to the total weighted average values.  $f = 90\% (\%)$  is commonly used to determine the effective sampling area for dielectric constant (Ferré *et al.* 1998).

The following steps are needed to use Eq. (11): Step 1) Calculate the the weighting function (Eq. (10)). This can be done by post-analyses of the results of electrical field distribution from Finite Element Analyses. Step 2) Calculate the denominator. It is calculated by the summation of value of the weighting function multiply the area of the elements (i.e.,  $s_i A_i$ ) on the whole computational domain. Step 3) Then, starting from areas with higher weighting function, the product of the weighing function and its area ( $w_i A_i$ ) is calculated. The product is continuously added together. When the summation is close to a certain percentage, for example 90%, of the denominator calculated from Step 2, the calculation stops. The effective sampling area consists of the areas included in the calculation so far.

Implementing the steps requires post-analyzing the results of by Finite Element Analyses (FEA). In this study, the results of electrical field distribution by FEA was explored. They are then analyzed by Matlab<sup>®</sup> code developed by the authors.

#### 2.2.4 Determination of the effective sampling area of TDR strip sensor by FEM simulations

The Poisson's equation is solved by use of the multi-physics software package COMSOL. The software offers powerful post processing functions to determine of the electrical field distribution and integration of the electrical field energy. The electric density distribution was exported from the FEM results. They are then analyzed using in-housed developed Matlab<sup>®</sup> code to determine the

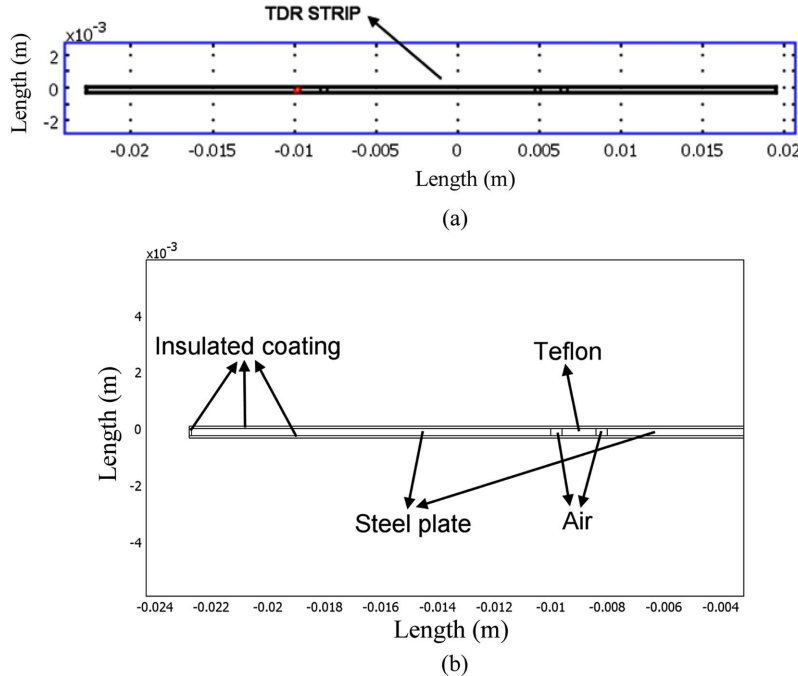


Fig. 7 (a) Schematic of the finite element model and (b) zoomed in on the left half of FEM model for the TDR strip

effective sampling area of the TDR strip.

The FEM model for the strip sensor is shown in Fig. 7(a). The model geometry is produced based on the actual geometry of the sensor strips. Fig. 7(b) is a close-up view on the strip. The coating is assumed to be made of a layer of plastic tape and a layer of adhesive. The dielectric constant of the tape is assumed to be 3. The dielectric constant of adhesive is assumed to be 7. The dielectric constant of Teflon is set to be 2.1 (Dielectric Properties of Polymers 2008). Ideally, the gaps between strips are filled with Teflon. In the actual fabrication, it is hard to cur Teflon strip with the exact width to fit the gap. Consequently, there are air gaps between the metallic strips. This is modeled by the FEM modeling (Fig. 7(b)). The dielectric constant of the air is set as 1.

To compute the electrical field distribution, a rectangular space surrounding the strip is included. A sensitivity study was performed in which the sizes the simulation zone were varied. It was found that as the size of the simulation zone increases, the electrical field distribution also changes. Theoretically the simulation zone should extend to infinite so that the boundary effects is eliminated. However, when the size of the simulation area is above certain area, there are only insignificant changes in the electrical field distribution. Large simulation zrea also comes with the cost of increasing computational time. Considering both the computational time and accuracy, the optimal simulation area selected is a 0.07 m by 0.03 m rectangular area. In the simulations, the electric potential at the center strip is set as 1 V and the electric potential at the outer strips is set as -1 V. The electric displacement at the outer rectangular boundary is set as 0.

Figs. 8(a) and 8(b) show the surface plot and the contour plot of the electric potential (voltage). The

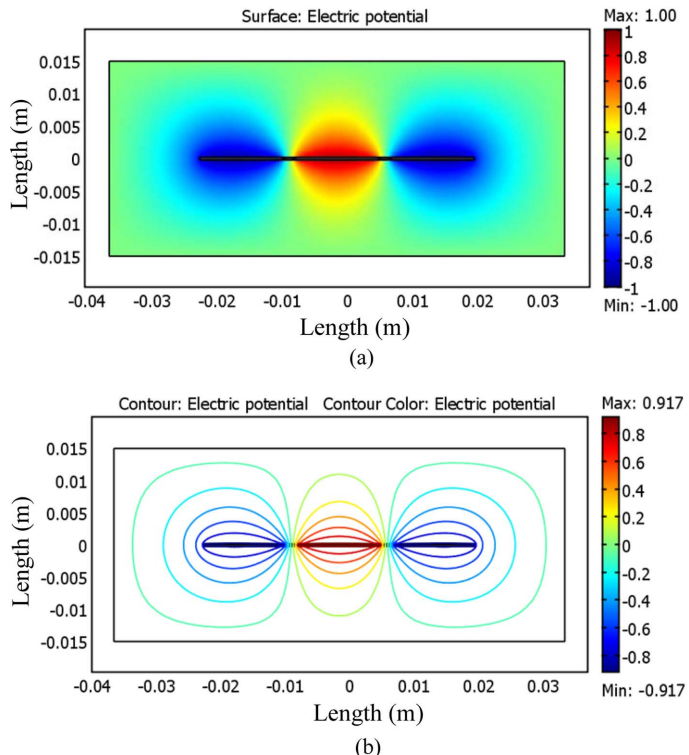


Fig. 8 (a) Surface plot of the electric potential in the electric field and (b) contour plot of the electric potential in the electric field

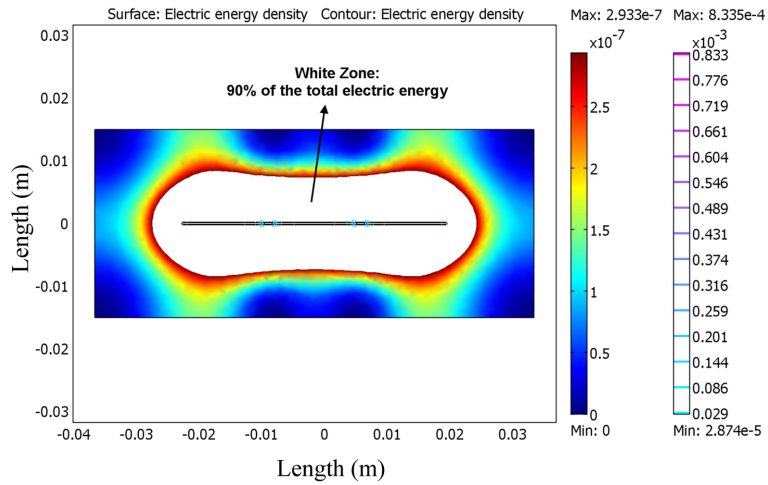


Fig. 9 The effective sampling zone (the white zone) by the strip sensor

highest energy-density occurs at the tips of the metal strip between the center strip and the outer strips.

The effective sampling area by the sensor strip can be determined using the accepted criterion (i.e., areas of electrical potential that make 90% of contribution to the total electrical field energy (Eq. (11))). This area is shown in Fig. 9. The effective sampling area extends around 1 cm in the direction perpendicular to the strip. This provides an effective sampling area of around  $10 \text{ cm}^2$  per unit length. The effective sampling area can be further increased for specific application purpose by modifying the sensor design, for example, by increasing the width of the sensor strip.

#### 2.2.5 Sensor calibration

A wooden box is used to calibrate the TDR strip sensor (Fig. 10). The size of wooden box is 268 mm $\times$ 165 mm $\times$ 120 mm. The box was cut in opposite sides. This allowed a section of TDR strip sensor to be placed across the box and subsequently backfilled with soil. Soil samples of different water content were prepared. At each water content, soil samples were placed into the box in layers and compacted until they completely fill the box. a TDR signal was taken. Afterwards, the water

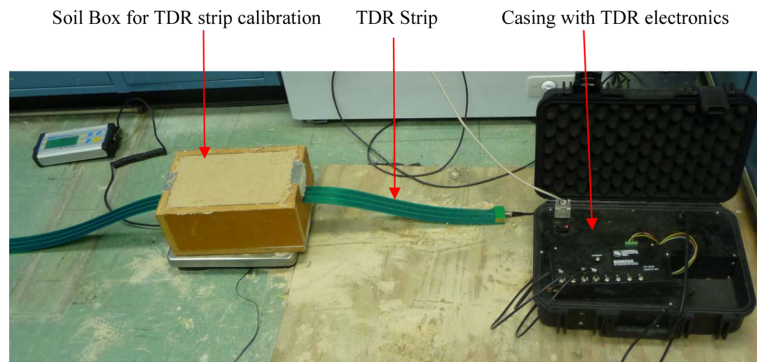


Fig. 10 Photo of calibration experiment for the TDR strip sensor

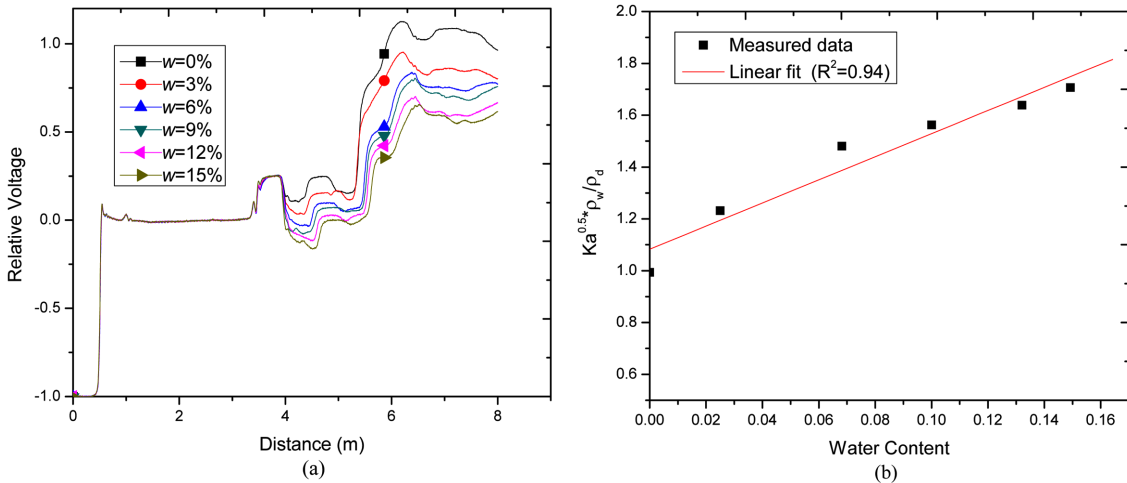


Fig. 11 (a) Measured TDR signals at different water content and (b) calibration of the measured dielectric constant by the strip sensor versus soil water content and density

content and density of soil were measured. Fig. 11(a) shows the measured TDR signals at different water contents. This figure shows a systematic trend of change as water content increases. This is an indication of the high sensitivity of this sensor to the moisture variations. The TDR signals were analyzed to determine the location of reflections using standard procedures proposed by Topp *et al.* (1980) and modified by Yu and Drnevich (2004). The dielectric constants were calculated from the travel distance.

The relationship between the water content, density and the dielectric constant measured by the TDR strip sensor are plotted in the format of equation developed by Siddiqui and Drnevich (1996), i.e., Eq. (3). Fig. 11(b) indicates there is good linear relationship between the dielectric constant measured by the strip sensor and the soil physical properties (such as the water content). The high linearity also means the soil physical properties can be accurately determined from the TDR measured dielectric constant. Since the TDR strip is uniformly aligned along the whole length. The calibration can be applied fro any section along the TDR strip.

### 3. Sensor installation

A critical requirement for the field monitoring sensor is they need to be able to survive the construction environment. Different modes of damage could result from construction activities, such as bending in the longitudinal or torsional directions, breakage of sensor strips due to tensional stresses. Both of these can happen when the construction equipment travels across sensor strip. These are less of a concern when the sensor is installed vertically. Compared with tradition rigid TDR sensors, this strip TDR sensor can accommodate significant amount of bending due to its high flexibility. Preliminary test results also indicate bending of the sensor strip up to 30 degrees does not significantly affect its performance (Yu, unpublished data). Besides, as no electronic component (such as impedance transform) is installed under the ground, the sensor is expected to be resistant to the construction loads.

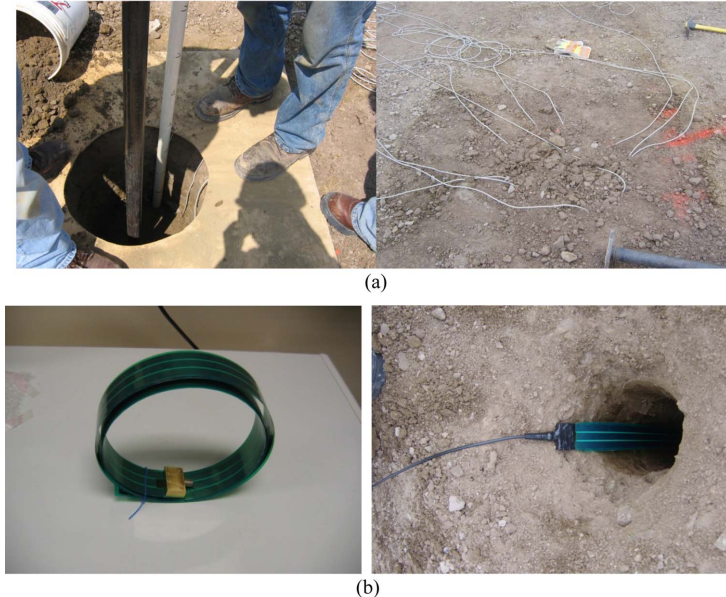


Fig. 12 (a) Installation of traditional TDR probes: left) drill hole; right) TDR cables and (b) installation of new TDR sensor: left) coiled TDR strip that is easy to carry; right) small hole for TDR strip sensor installation

The TDR strip sensor was installed at a test site on route 23 near the Delaware State Park in Ohio. This provides an opportunity to compare the performance of the developed TDR strip sensor with conventional TDR moisture sensors. Based on the field experience, advantages of this strip sensor are identified.

- 1) Mobility. The TDR strip sensor can be coiled and is easy to carry (Fig. 12(b)).
  - 2) Installation requirement. The traditional TDR probes required drilling a hole with diameter of at least one foot, while the TDR strip required a hole of less than three inches. This means less extent of soil disturbance and less dependent on machine power for installation (Figs. 12(a), 12(b)).
  - 3) Cable: With traditional TDR probes, plural number of cables and data acquisition (DAQ) ports are needed to monitor the spatial moisture distribution. In comparison, the TDR strip sensor only needs one cable and one DAQ port due to the distributed moisture sensing capability.
  - 4) Labor: From our field experience, the installation of this new strip TDR sensor only took around 1/3~1/5 of the time required to install the traditional TDR sensors.
- These comparisons clearly demonstrate the advantages of this new TDR sensor over the traditional TDR probes.

#### 4. Conceptual evaluation of sensor applications

Simulated experiments were conducted to determine the capability and sensitivity of the developed TDR strip sensor to the subsurface moisture migration processes.

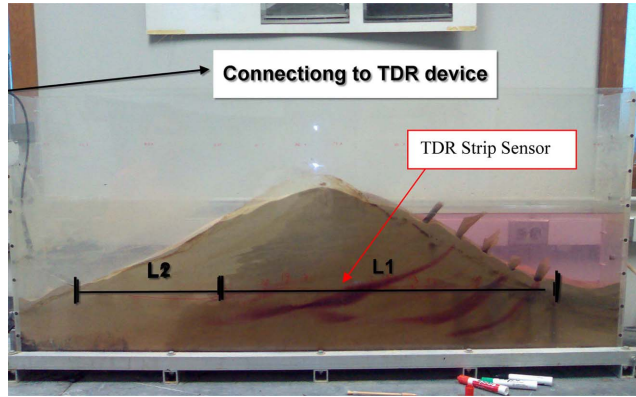


Fig. 13 Photo of the sand tank seepage monitoring

#### 4.1 Monitoring of seepage in model embankment

Seepage and consequent piping is a major factor affecting the safety of levees and earth dams. Simulation experiments were conducted to evaluate the performance of TDR strip sensor to monitor the seepage process. The evaluation was conducted in a model tank (Fig. 13). The model embankment was constructed of an ASTM standard fine sand with particle sizes ranging between 0.074 mm to 0.42 mm. The strip was buried in the model embankment in the horizontal direction along the black line shown in this figure. After the sensor was installed, water was filled in the right hand side of the model levee to initialize the seepage process. TDR signals were automatically taken by in-house developed computer software at given time intervals. The locations of seepage front at corresponding time are also directly observed and recorded.

Examples of recorded TDR signals by the strip sensor are shown in Fig. 14(a). There was a stagnant period in seepage initialization during the first four minutes (when water is being filled on

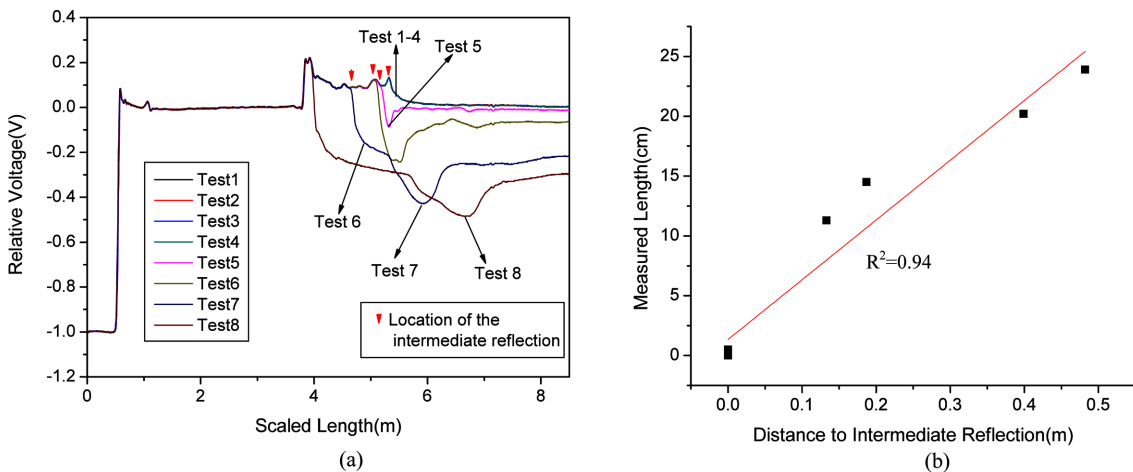


Fig. 14 (a) Measured TDR signals during the seepage experiment and (b) relationship between the distance of seepage wet front and the distance to intermediate reflection  
 (Note: Test 1-4: 1, 2, 3, 4 minutes respectively after the experiment start, Test 5, 6, 7, 8: 9, 14, 19, 24, 29 minutes respectively after the experiment start)

the upstream of the model levee). This is also seen from TDR signals 1-4 in Fig. 14(a). After that, there are appreciable amount of progresses in the wet front migration. This can be identified from the reflections marked on the TDR signals in Fig. 14(a). Fig. 14(b) plots the manually measured wet front location and the distance to intermediate reflection. Very good linear relationship is observed between both quantities. This indicates the TDR strip sensor can accurately detect the location of wet front, which qualifies it for monitoring of seepage across levee and earth embankment. Details on the spatial distribution of moisture can be determined by use of advanced analyses procedures that are under further development.

#### 4.2 Monitoring the water infiltration

Determining the amount and progresses of water infiltration is important for disciplines such as Water Resources and Soil Sciences. A translucent tube is used to evaluate the performance of this TDR strip sensor for monitoring the water infiltration process. The transparent tube helps to directly observe the progresses of water infiltration. The TDR strip sensor was first aligned in the middle of the tube. Soil (fine sand) was carefully compacted around the strip to a preset height. The strip sensor was connected to TDR electronics via a coaxial cable. After the monitoring software is activated, water is sprayed on surface of sand column to initialize the precipitation process. The progresses of observed infiltration front were also manually measured and recorded. The experiment lasted for about fifty minutes.

A few geometries were noted in the model tube in Fig. 15. L1 is the depth of the wet front due to the simulated precipitation, L2 stands for the depth of the dry sand column, and L3 is the height of observed capillary rise at the bottom of sand column.

Example of measured signals during the water infiltration process was plotted in Fig. 16(a). Signals at different times are plotted to show the trend of changes. The signal denoted as Test 1 is the first signal obtained when the experiment started. Time when the other signals were acquired is also noted in this figure. The general trend is that as the wet front progresses, it takes longer time to receive the TDR returning signals. This group of signals clearly show the systematic change in location of the intermediate reflections in the TDR signals (Fig. 16(a)).

Fig. 16(b) plots the location of intermediate reflection on the TDR signal versus the measured

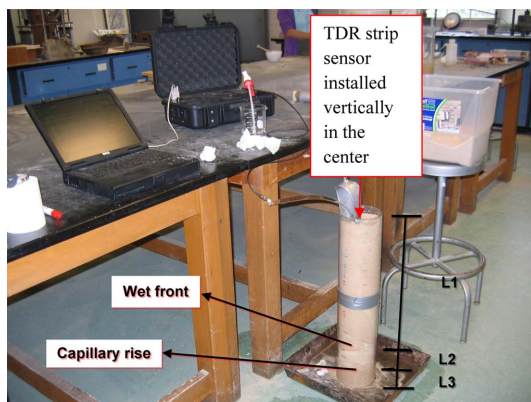


Fig. 15 Test set up for monitoring the precipitation process

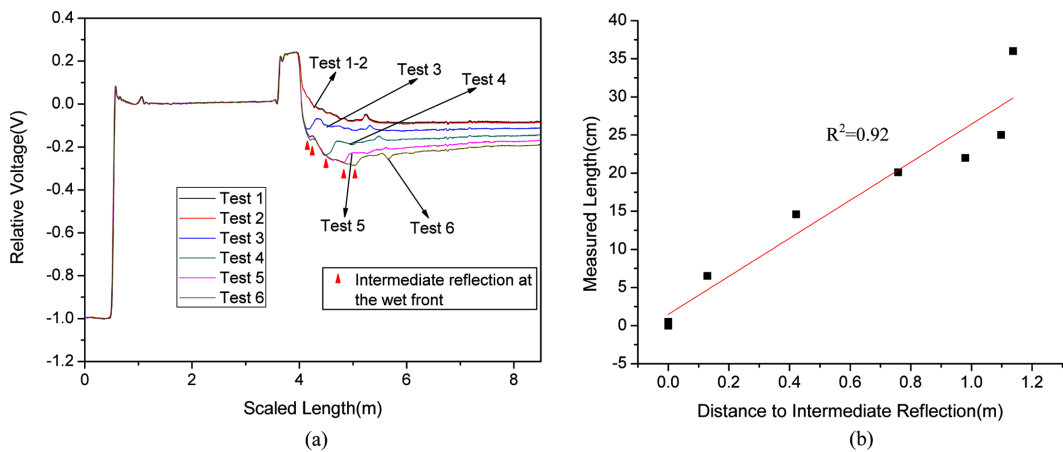


Fig. 16 (a) Measured TDR signals during the precipitation test and (b) relationship between the manually measured infiltration depth and the distance to intermediate reflection from TDR signals  
 (Note: Test 1-2: 1, 2 minutes respectively after the experiment start, Test 3, 4, 5, 6: 7, 12, 17, 22 minutes respectively after the experiment start)

depth of infiltration. There is a good linear correlation between these quantities. This indicates that this TDR strip sensor can monitor the progress of infiltration.

## 5. Conclusions

An innovative TDR strip sensor has been designed and fabricated to measure the subsurface moisture distribution. It is sensitive, inexpensive, rugged and easily deployed. FEM simulation was performed to determine the electric field distribution around the metallic waveguide. The effective measurement range was determined based on FEM results. Results of calibration experiments show this TDR strip sensor has high accuracy for water content estimation. The sensor performance was evaluated in simulated experiments, all showing promising results. Experience of field installation indicates this new sensor has many advantages over the traditional monitoring probes. With further improvement in the sensor design, this innovative sensor will be a useful tool for monitoring the infrastructure performance.

## Acknowledgements

The authors would like to thank Roger Green of the Ohio Department of Transportation for his help and encouragement to pursue this innovation. The assistance of ODOT drilling crews during field installation is also highly appreciated.

## References

- Abo-Hashema, M.A., Bayomy, F.M., Smith, R. and Salem, H.M. (2002), "Environmental impacts on subgrade resilient modulus for Idaho pavements", *Proceedings of the Transportation Research Board (TRB) 81st Annual*

- Meeting*, Washington D.C., DC, USA, January.
- Baker, J.M. and Allmaras, R.R. (1990), "System for automating and multiplexing soil moisture measurement by time-domain reflectometry", *Soil Sci. Soc. Am. J.*, **54**(1), 1-6.
- Campbell, C.G., Ghodrati, M. and Garrido, F. (1999), "Comparison of time domain reflectometry, fiber optic mini-probes, and solution samplers for real time measurements of solute transport in soil", *Soil Sci.*, **164**(3), 156-170.
- Chen, G., Mu, H.M., Pommerenke, D. and Drewniak, J.L. (2004), "Damage detection of reinforced concrete beams with novel distributed crack/strain sensors", *Struct. Health Monit.*, **3**(3), 225-243.
- Drnevich, V.P., Lin, C.P., Yi, Q., Yu, X. and Lovell, J. (2001a), *Realtime determination of soil type, water content and density using electromagnetics*, Final Report FHWA/IN/JTRP-2000/20, Joint Transportation Research Program, School of Civil Engineering, Purdue University, West Lafayette, IN, USA, <http://docs.lib.purdue.edu/cgi/viewcontent.cgi?article=1648&context=jtrp>.
- Drnevich, V.P., Siddiqui, S.I., Lovell, J. and Yi, Q. (2001b), "Water content and density of soil insitu by the Purdue TDR method", *Proceedings of the TDR2001 International Conference*, Northwestern University, Evanston, IL, USA, September.
- Ferré, P.A., Knight, J.H., Rudolph, D.L. and Kachanowski, R.G. (1998), "The sample areas of conventional and alternative time domain reflectometry probes", *Water Resour. Res.*, **34**(11), 2971-2979.
- Graf, J. and Zink, S. (2005), "Patching problems: often what caused the pavement failure lies not on the surface, but with the subgrade", *HMAT*, **10**(2), 47-48.
- Heimovaara, T.J. (1994), "Frequency domain analysis of time domain reflectometry waveforms: 1.Measurement of the complex dielectric permittivity of soils", *Water Resour. Res.*, **30**(2), 189-199.
- Hong, G.T., Bulut, R., Aubeny, C.P., Jayatilaka, R. and Lytton, R.L. (2006), "Prediction of roughness of pavements on expansive soils", *Proceedings of the Fourth International Conference on Unsaturated Soils*, (Eds. Gerald A. Miller, Claudia E. Zapata, Sandra L. Houston and Delwyn G. Fredlund), Carefree, AZ, USA, April.
- Huang, Y.H. (2003), *Pavement Analysis and Design*, 2nd Ed., Prentice Hall.
- Knight, J.H. (1992), "Sensitivity of time domain reflectometry measurements to lateral variations in soil water content", *Water Resour. Res.*, **28**(9), 2345-2352.
- Lin, M.W., Abatan, A.O. and Danjaji, M.B. (1997), "Electrical time domain reflectometry sensing cables as distributed stress/strain sensors in smart materials systems", *Proc. SPIE*, **3042**, 33-44.
- Lin, M.W., Thaduri, J. and Abatan, A.O. (2005), "Development of an electrical time domain reflectometry (ETDR) distributed strain sensor", *Meas. Sci. Technol.*, **16**(7), 1495-1505.
- Liang, R.Y., Al-Akhras, K. and Rabab'ah, S. (2006), "Field monitoring of moisture variations under flexible pavement", *Proceedings of the 2006 TRB 85th Annual Meeting*, Washington D.C., DC, USA, January.
- Mojid, M.A., Wyseure, G.C.L. and Rose, D.A. (1998), "The use of insulated time-domain reflectrometry sensors to measure water content in highly saline soils", *Irrigation Sci.*, **18**(2), 55-61.
- Nichol, C., Beckie, R. and Smith, L. (2002), "Evaluation of uncoated and coated time domain reflectometry probes for high electrical conductivity systems", *Soil Sci. Soc. Am. J.*, **66**(5), 1454-1465.
- O'Connor, K.M. and Dowding, C.H. (1999), *GeoMeasurements by Pulsing TDR Cables and Probes*, CRC Press, USA.
- Persson, M., Bendz, D. and Flyhammar, P. (2004), "Time-domain reflectometry probe for water content and electrical conductivity measurements in saline porous media", *Vadose Zone J.*, **3**(4), 1146-1151.
- Ramo, S., Whinnery, J.R. and Van Duzer, T. (1994), *Fields and waves in communication electronics*, John Wiley and Sons, New York.
- Salem, R.M., Burdette, E.G. and Jackson, N.M. (2003), "Resistance to freezing and thawing of recycled aggregate concrete", *ACI Mater. J.*, **100**(3), 216-221.
- Schlaeger, S., Huebner, C., Scheuermann, A. and Gottlieb, J. (2001), "Development and application of TDR inversion algorithms with high spatial resolution for moisture profile determination", *Proceedings of the Second International Symposium and Workshop on Time Domain Reflectometry for Innovative Geotechnical Applications*, Northwestern University, Evanston, IL, USA, September.
- Siddiqui, S.I. and Drnevich, V.P. (1995), *Use of time domain reflectometry for the determination of water content and density of soil*, Final Report FHWA/IN/JHRP-95/9, Joint Highway Research Project, School of Civil Engineering, Purdue University, West Lafayette, IN, USA.

- Siddiqui, S.I. and Drnevich, V.P. (1996), *A new method of measuring density and moisture content of soil using the technique of time domain reflectometry*, Report No. FHWA/IN/JTRP-95/9, Joint Transportation Research Program, Indiana Department of Transportation, Purdue University, West Lafayette.
- Stastny, J.A., Rogers, C.A. and Liang, C. (1993), "Distributed electrical time domain reflectometry (ETDR) structural sensors: design models and proof-of-concept experiments", *Proc. SPIE*, **1918**, 366-376.
- Sun, Z.J., Young, G.D., McFarlane, R.A. and Chambers, B.M. (2000), "The effect of soil electrical conductivity on moisture determination using time-domain reflectometry in sandy soil", *Can. J. Soil Sci.*, **80**(1), 13-22.
- Tang, L.Q., Tao, X.M. and Choy, C.L. (2001), "Possibility of using a coaxial cable as a distributed strain sensor by time domain reflectometry", *Smart Mater. Struct.*, **10**(2), 221-228.
- Topp, G.C., Davis, J.L. and Annan, A.P. (1980), "Electromagnetic determination of soil water content: measurements in coaxial transmission lines", *Water Resour. Res.*, **16**(3), 574-582.
- Topp, G.C. and Davis, J.L. (1985), "Measurement of soil water content using time domain reflectometry (TDR): A field evaluation1", *Soil Sci. Soc. Am. J.*, **49**(1), 19-24.
- Wörsching, H., Becker, R., Schlaeger, S., Bieberstein, A. and Kudella, P. (2006), "Spatial-TDR moisture measurement in a large scale Levee model made of Loamy soil material", *Proceedings of the TDR 2006: Third International Symposium and Workshop on Time Domain Reflectometry for Innovative Soils Applications*, Purdue University, IN, USA, September.
- Yu, X. (2003), *Influence of Soil Properties and Environmental Conditions on Electromagnetic Wave Propagation in Soils*, Ph.D. Thesis, School of Civil Engineering, Purdue University.
- Yu, X. and Drnevich, V.P. (2004), "Soil water content and dry density by time domain reflectometry", *J. Geotech. Geoenvir. Eng.*, **130**(9), 922-934.
- Yu, X. and Yu, X. (2006), "Time domain reflectometry tests of multilayered soils", *Proceedings of the TDR 2006: Third International Symposium and Workshop on Time Domain Reflectometry for Innovative Soils Applications*, Purdue University, IN, USA, September.
- Zegelin, S.J., White, I. and Jenkins, D.R. (1989), "Improved field probes for soil water content and electrical conductivity measurement using time domain reflectometry", *Water Resour. Res.*, **25**(11), 2367-2376.

CC